Bose-Einstein Condensation of ^{84}Sr

Y. N. Martinez de Escobar, P. G. Mickelson, M. Yan, B. J. DeSalvo, S. B. Nagel, and T. C. Killian

Rice University, Department of Physics and Astronomy, Houston, Texas 77251, USA

(Received 15 October 2009; published 9 November 2009)

We report Bose-Einstein condensation of ^{84}Sr in an optical dipole trap. Efficient laser cooling on the narrow intercombination line and an ideal s-wave scattering length allow the creation of large condensates ($N_0 \sim 3 \times 10^5$) even though the natural abundance of this isotope is only 0.6%. Condensation is heralded by the emergence of a low-velocity component in time-of-flight images.

DOI: 10.1103/PhysRevLett.103.200402 PACS numbers: 03.75.Hh, 67.85.Hj

The study of quantum degenerate gases continues to be at the forefront of research in atomic and condensed matter physics nearly 15 years after the first observation of Bose-Einstein condensation [1–3]. Current areas of focus include the behavior of quantum fluids in optical lattices [4], effects of dimensionality [5] and disorder [6,7], exploration of the BEC-BCS crossover regime [8], and the pursuit of quantum degenerate molecular systems [9].

Quantum degeneracy in alkaline earth metal atoms and atoms with similar electron structure has become another area of intense activity. These systems have been the subject of many recent theoretical proposals for quantum computing in optical lattices [10–12] and creation of novel quantum fluids [13]. They possess interesting and useful collisional properties, such as a wealth of isotopes that allow mass tuning of interactions [14,15] and creation of various quantum mixtures [16]. Low-loss optical Feshbach resonances [17–19] in these atoms promise new opportunities because they enable changing the atomic scattering lengths on small spatial and temporal scales. This can lead to creation of matter-wave solitons in two dimensions [20] and random nonlinear interactions in quantum fluids [21]. Many of these ideas take advantage of the existence of long-lived metastable triplet states and associated narrow optical transitions, which are also the basis for recent spectacular advances in optical frequency metrology [22].

Here we report the observation of Bose-Einstein condensation of ^{84}Sr. To date, all-optical formation [23] of quantum degeneracy with alkaline earth metal atoms and similar elements has been reported in a collection of ytterbium isotopes [16,24–26], and very recently in ^{40}Ca [27] and ^{84}Sr [28], demonstrating increasing interest in these systems. Starting with a natural-abundance strontium source, our success in forming a relatively large Bose-Einstein condensate of ^{84}Sr, which has a natural abundance of 0.6%, demonstrates the power of laser cooling in strontium using the $(5s^2)^1S_0 - (5s5p)^3P_1$ narrow intercombination line at 689 nm [29]. It also reflects the near-ideal scattering properties of this isotope, which has an s-wave elastic scattering length of $a = 122.7(3)a_0$ [15], where $a_0 = 0.53$ Å. The ground-state scattering properties of all Sr isotopes are well characterized from one- [30–32] and two-photon [15] photoassociative spectroscopy, Fourier transform molecular spectroscopy [33], and experiments trapping various isotopes in optical traps [34,35].

The apparatus and experimental sequence for laser cooling atoms and loading them into our optical dipole trap (ODT) were described in [15,36,37], and a timing diagram is shown in Fig. 1. Several techniques are used to enhance initial number and subsequent transfers to overcome the low abundance of ^{84}Sr. We form an atomic beam and utilize two-dimensional (2D) collimation and Zeeman cooling to load a magneto-optical trap (MOT), all using the $(5s^2)^1S_0 - (5s5p)^1P_1$ transition at 461 nm. The MOT consists of three retroreflected beams, each with peak intensity of 3.6 mW/cm^2 and red detuned from atomic resonance by 60 MHz.

One in 10^5 $(5s5p)^1P_1$ atoms decays to the $(5s4d)^1D_2$ level and then to the $(5s5p)^3P_1$ and $(5s5p)^3P_2$ states. $(5s5p)^3P_1$ atoms return to the ground state and are recaptured in the MOT, but a fraction of $(5s5p)^3P_2$ atoms, with a lifetime of 9 min [38], are trapped in the quadrupole magnetic field of the MOT [36,37,39]. We can accumulate 2.5×10^7 atoms in an axial magnetic field gradient of 60 G/cm with 30 s of loading. $(5s5p)^3P_2$ atoms are then

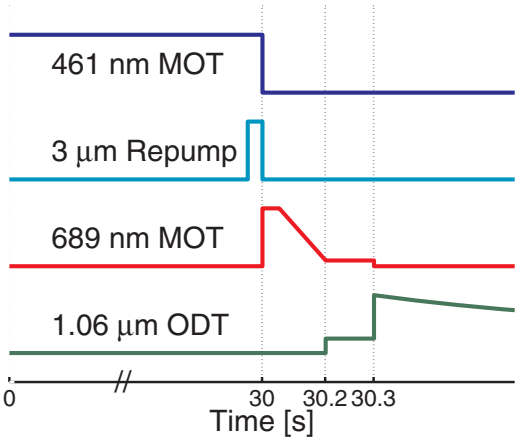

FIG. 1 (color online). Timing diagram for principal experimental components. The traces are offset for clarity and heights schematically indicate variation in power. Note the break in the time axis.

returned to the 461 nm cycling transition by repumping for 35 ms via the $(5s5p)^3P_2 - (5s4d)^3D_2$ transition at 3012 nm [37]. We subsequently reduce the 461 nm beam intensities to about 0.36 mW/cm^2 for 6.5 ms to reduce the sample temperature to 2 mK.

The 461 nm light is then extinguished, and a second stage of cooling begins using the 689 nm $(5s^2)^1S_0 - (5s5p)^3P_1$ intercombination line. This MOT light, consisting of three retroreflected beams with 2 cm diameters, is initially red detuned 1 MHz from resonance and broadened by 700 kHz (peak-to-peak dither amplitude) to enhance our 689 nm MOT capture rate. The peak intensity is 0.75 mW/cm^2 per beam, and the magnetic quadrupole field gradient is 0.1 G/cm. Over the next 150 ms, the field gradient is increased to 0.8 G/cm, the laser spectrum is reduced to single frequency and detuned by only ~30 kHz, and the power is reduced to 0.15 mW/cm^2. This results in 1.6×10^7 atoms at a temperature of 1 μK and a peak density of $\sim 10^{12}$ cm^{-3}. The transfer efficiency into the intercombination line MOT decreases significantly with larger numbers of atoms, which are obtainable with other isotopes. This is consistent with two-body light assisted losses being the dominant loss process [40].

Our ODT, consisting of two crossed beams, is then overlapped with the intercombination line MOT for 115 ms with modest power (2.5 W) per beam. The ODT is formed by a single beam derived from a 20 W multimode, 1.06 μm fiber laser that is recycled through the chamber. The beams cross nearly perpendicularly, but the plane of the lasers is inclined by approximately 10.5° from horizontal. This results in a trap with equipotentials that are nearly oblate spheroids, with the tight axis close to vertical. Each beam has a waist of approximately 100 μm in the trapping region. This is slightly different than other realizations of quantum degeneracy in two-electron atoms, in which at least one beam had a waist that was significantly smaller [16,24,25,27,28].

Immediately after extinction of the 689 nm light, the ODT power is ramped to 10 W in 20 ms to obtain a sample of 3×10^6 atoms at 5 μK. The trap depth is 31 μK, and the peak density at this point is 4×10^{13} cm^{-3}, which implies an average collision rate of 1000 s^{-1}. The peak phase space density (PSD) is 10^{-2}. For diagnostics, we record absorption images of samples released from the trap after a time of flight varying from 10 to 40 ms, and the optical depth profile can be related to the areal density, which, for these long delays, also provides the velocity distribution.

Figure 2 shows the number, temperature, and phase space density evolution for a typical forced evaporation trajectory. We ramp down the power in the lasers according to $P = P_0/(1 + t/\tau)^\beta$, with time denoted by t, $\beta = 1.5$, and $\tau = 1.5$ s. This trajectory is designed to approximately maintain a constant ratio of trap depth to temperature (η) during evaporation [41]. The lifetime of atoms in the ODT is 30 s, limited primarily by background gas collisions.

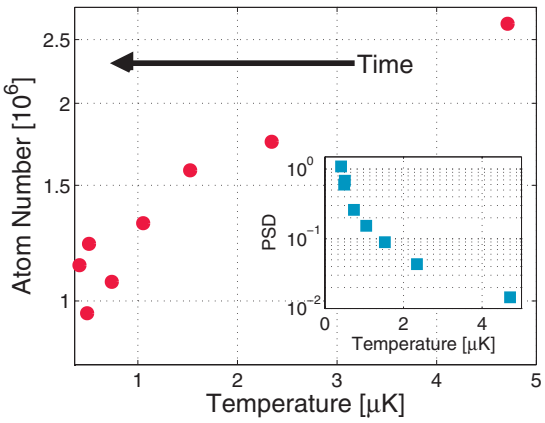

FIG. 2 (color online). Number, temperature, and phase space density along a typical evaporation trajectory, from 200 ms after the completion of loading of the optical dipole trap and commencement of evaporation, until quantum degeneracy is reached 3 s later. The phase space density increases by a factor of 100 for a reduction of atom number by a factor of 3.

This allows efficient evaporation at a measured $\eta = 8 \pm 1$ for most of the trajectory.

After 3 s of evaporation to a power of 2 W, 1×10^6 atoms remain at a temperature of 0.4 μK. For this trap, our measured trap oscillation frequencies [42] yield a trap depth, including the effect of gravity, of 3.5 ± 0.3 μK and a mean trap frequency of $\bar{f} = (f_x f_y f_z)^{1/3} = 84 \pm 5$ Hz. These values indicate that the sample is at the critical transition temperature for a harmonic trap [43],

$$T_c = \frac{1}{k_B} \frac{\hbar \bar{\omega} N^{1/3}}{\zeta(3)}, \quad (1)$$

at which the PSD is 1.2, where N is the number of trapped atoms, k_B is Boltzmann's constant, $\hbar$ is the reduced Planck constant, $\bar{\omega}$ is $2\pi\bar{f}$, and ζ is the Riemann zeta function.

The evaporation is quite efficient. We lose a factor of 3 in the number of atoms from initiation of forced evaporation to the onset of degeneracy, while the phase space density increases by about a factor of 100. The predicted scaling $\rho/\rho_i = (N_i/N)^{\eta'-4}$ [41], where ρ_i and N_i are the initial phase space density and number, and $\eta' = \eta + (\eta - 5)/(\eta - 4)$, implies that $\eta = 7.5$, in excellent agreement with our estimate from knowledge of the optical trap parameters and measured sample temperature.

Figure 3 shows false color 2D rendering and 1D slices through the time-of-flight images recorded after 38 ms of expansion for various points along the evaporation trajectory. At 2.7 s of evaporation, the distribution is fit well by a Boltzmann distribution, but at 3 s, the presence of a Bose-Einstein condensate is indicated by the emergence of a narrow peak at low velocity. Further evaporation to a beam power of 1.3 W at 4.35 s and trap depth of 600 nK yields a condensate with a negligible thermal fraction.

The areal density of expanded condensates is fit with the functional form [44]

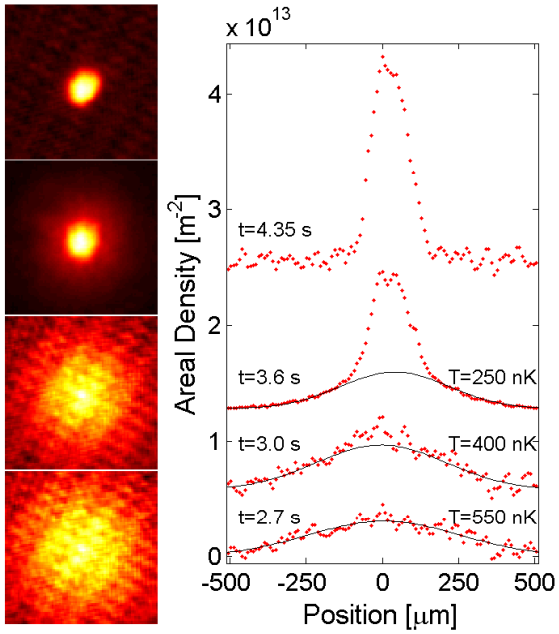

FIG. 3 (color online). Appearance of Bose-Einstein condensation in absorption images (left) and areal density profiles (right). Data correspond to 35 ms of free expansion after indicated evaporation times, t. (left) Images are 780 μm per side, and have the same time stamp as the density profiles. (right) The areal density profiles are from a vertical cut through the center of the atom cloud, and temperatures are extracted from 2D Gaussian fits to the thermal component. At 3.0 and 3.6 s, a bimodal distribution indicative of Bose-Einstein condensation becomes increasingly clear, and then a pure condensate is shown at 4.35 s.

$$n(x,y) = \frac{5N_0}{2\pi R_x R_y}\left(1-\frac{x^2}{R_x^2}-\frac{y^2}{R_y^2}\right)^{3/2}\theta\left(1-\frac{x^2}{R_x^2}-\frac{y^2}{R_y^2}\right), \quad (2)$$

where θ is the Heaviside function, and R_x and R_y are the condensate radii. At 600 nK trap depth, fitting the areal density yields typical values of $N_0 = 3.0 \times 10^5$ for the largest condensates. The trap mean oscillation frequency at this point is $\bar{f} = 70$ Hz and the harmonic oscillator length is $a_{\rm ho} = [\hbar/(m\bar{\omega})]^{1/2} = 1.3$ μm, where m is the atomic mass. The trap harmonic oscillator energy scale is $\hbar\bar{\omega}/k_B = 3.3$ nK and the chemical potential is $\mu = \frac{\hbar\bar{\omega}}{2k_B} \times (\frac{15N_0a}{a_{\rm ho}})^{2/5} = 90$ nK. $(N_0a)/a_{\rm ho} = 1500$ is large, implying that the condensate is in the strong interaction regime and should be well described by a Thomas-Fermi density distribution, confirming that Eq. (2) is the appropriate description.

By releasing a pure condensate from the trap and varying the time of flight before recording an absorption image, we are able to characterize the expansion of the many-body wave function which is sensitive to the chemical potential and confinement of the trapped sample. Figure 4 shows the evolution of condensate radii as a function of expansion time obtained by fitting the optical depth to Eq. (2). The fitting coordinate system has been rotated to align with the principal axes of the condensate. These samples contain $N_0 = 2.3 \times 10^5$ atoms and were obtained after 4.5 s of evaporation to an estimated trap depth of 350 nK and trap frequencies of 90 Hz close to vertical and 60 Hz along the perpendicular axes. The radii show an inversion, as expected for an expanding condensate, but the effect is small because the trap is not highly asymmetric.

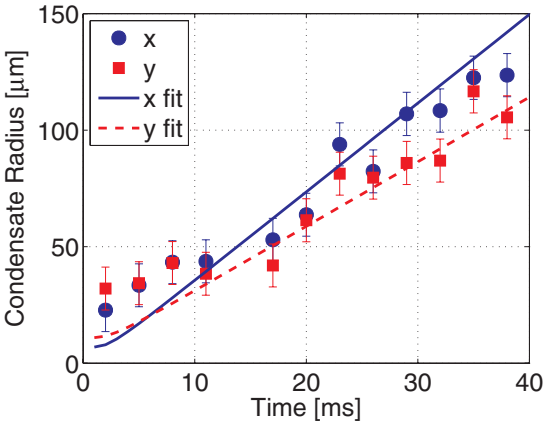

FIG. 4 (color online). Condensate radius after release from the trap. The expansion of the condensate is fit by the Castin-Dum model [Eq. (3)] assuming trap parameters obtained from profiling the ODT beam and measuring the trap oscillation frequencies. Deviations at early times most likely reflect limitations of the optical imaging system and large optical depth of the condensate.

We fit the data using a numerical solution of the Castin-Dum model [45] for the free expansion of a Thomas-Fermi wave function [44]. The radii evolve according to

$$R_i(t) = R_i(0)b_i(t) = \sqrt{\frac{2\mu}{m(2\pi f_i)^2}}b_i(t) \quad (3)$$

for $i = x, y, z$, where the scaling parameters obey $\ddot{b}_i = (2\pi f_i)^2/(b_i b_x b_y b_z)$. Using the well-known value of the scattering length [15] and our estimated trap parameters

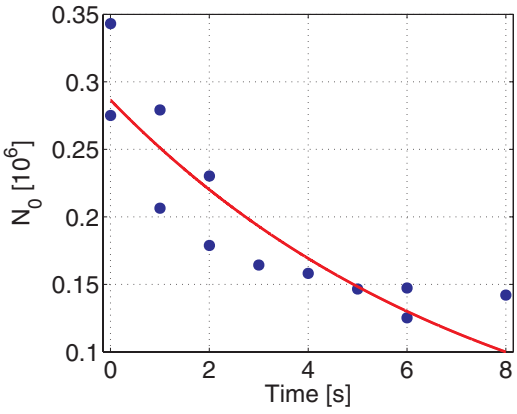

FIG. 5 (color online). Number of condensate atoms held in the optical dipole trap at constant depth versus time after the evaporation (see text). The solid line is an exponential fit to the data, yielding a condensate lifetime of 8 ± 1 s.

obtained from beam profiling and trap oscillation frequency measurements, we obtain a good fit to the measured expansion.

If, instead of releasing the condensate from the trap, the trap is held constant after 4.5 s of evaporation, the lifetime of the condensate can be measured. Figure 5 shows a fit of the decay to an exponential, yielding a lifetime of 8 ± 1 s. No discernible thermal fraction was evident in these samples.

The large number of condensate atoms and the long sample lifetime indicate favorable conditions for many experiments. Of particular interest in the near future are the achievement of quantum degeneracy with other strontium isotopes and mixtures, and the application of an optical Feshbach resonance to a quantum degenerate sample.

We thank F. Schreck for helpful discussions and F. Tittel for the loan of crucial equipment. This research was supported by the Welch Foundation (C-1579), the National Science Foundation (PHY-0855642), and the Keck Foundation.

[1] C. C. Bradley, C. A. Sackett, J. J. Tollett, and R. G. Hulet, Phys. Rev. Lett. **75**, 1687 (1995).
[2] M. H. Anderson, J. R. Ensher, M. R. Matthews, C. E. Wieman, and E. A. Cornell, Science **269**, 198 (1995).
[3] K. B. Davis, M. O. Mewes, M. R. Andrews, N. J. van Druten, D. S. Durfee, D. M. Kurn, and W. Ketterle, Phys. Rev. Lett. **75**, 3969 (1995).
[4] M. Greiner and S. Folling, Nature (London) **453**, 736 (2008).
[5] A. Görlitz *et al.*, Phys. Rev. Lett. **87**, 130402 (2001).
[6] J. Billy *et al.*, Nature (London) **453**, 891 (2008).
[7] G. Roati *et al.*, Nature (London) **453**, 895 (2008).
[8] I. Bloch, J. Dalibard, and W. Zwerger, Rev. Mod. Phys. **80**, 885 (2008).
[9] K.-K. Ni, S. Ospelkaus, M. H. G. de Miranda, A. Pe'er, B. Neyenhuis, J. J. Zirbel, S. Kotochigova, P. S. Julienne, D. S. Jin, and J. Ye, Science **322**, 231 (2008).
[10] A. J. Daley, M. M. Boyd, J. Ye, and P. Zoller, Phys. Rev. Lett. **101**, 170504 (2008).
[11] A. V. Gorshkov, A. M. Rey, A. J. Daley, M. M. Boyd, J. Ye, P. Zoller, and M. D. Lukin, Phys. Rev. Lett. **102**, 110503 (2009).
[12] I. Reichenbach, P. S. Julienne, and I. H. Deutsch, Phys. Rev. A **80**, 020701(R) (2009).
[13] M. Hermele, V. Gurarie, and A. M. Rey, Phys. Rev. Lett. **103**, 135301 (2009).
[14] M. Kitagawa, K. Enomoto, K. Kasa, Y. Takahashi, R. Ciurylo, P. Naidon, and P. S. Julienne, Phys. Rev. A **77**, 012719 (2008).
[15] Y. N. Martinez de Escobar, P. G. Mickelson, P. Pellegrini, S. B. Nagel, A. Traverso, M. Yan, R. Côté, and T. C. Killian, Phys. Rev. A **78**, 062708 (2008).
[16] T. Fukuhara, S. Sugawa, Y. Takasu, and Y. Takahashi, Phys. Rev. A **79**, 021601(R) (2009).
[17] R. Ciurylo, E. Tiesinga, and P. S. Julienne, Phys. Rev. A **71**, 030701(R) (2005).
[18] K. Enomoto, K. Kasa, M. Kitagawa, and Y. Takahashi, Phys. Rev. Lett. **101**, 203201 (2008).
[19] Y. N. Martinez de Escobar, P. G. Mickelson, M. Yan, and T. C. Killian, arXiv:0906.1837.
[20] H. Saito and M. Ueda, Phys. Rev. Lett. **90**, 040403 (2003).
[21] M. P. A. Fisher, P. B. Weichman, G. Grinstein, and D. S. Fisher, Phys. Rev. B **40**, 546 (1989).
[22] J. Ye, H. J. Kimble, and H. Katori, Science **320**, 1734 (2008).
[23] M. D. Barrett, J. A. Sauer, and M. S. Chapman, Phys. Rev. Lett. **87**, 010404 (2001).
[24] T. Fukuhara, Y. Takasu, M. Kumakura, and Y. Takahashi, Phys. Rev. Lett. **98**, 030401 (2007).
[25] T. Fukuhara, S. Sugawa, and Y. Takahashi, Phys. Rev. A **76**, 051604(R) (2007).
[26] Y. Takasu, K. Maki, K. Komori, T. Takano, K. Honda, M. Kumakura, T. Yabuzaki, and Y. Takahashi, Phys. Rev. Lett. **91**, 040404 (2003).
[27] S. Kraft, F. Vogt, O. Appel, F. Riehle, and U. Sterr, Phys. Rev. Lett. **103**, 130401 (2009).
[28] S. Stellmer, M. K. Tey, B. Huang, R. Grimm, and F. Schreck, preceding Letter, Phys. Rev. Lett. **103**, 200401 (2009).
[29] H. Katori, T. Ido, Y. Isoya, and M. Kuwata-Gonokami, Phys. Rev. Lett. **82**, 1116 (1999).
[30] S. B. Nagel, P. G. Mickelson, A. D. Saenz, Y. N. Martinez, Y. C. Chen, T. C. Killian, P. Pellegrini, and R. Côté, Phys. Rev. Lett. **94**, 083004 (2005).
[31] P. G. Mickelson, Y. N. Martinez, A. D. Saenz, S. B. Nagel, Y. C. Chen, T. C. Killian, P. Pellegrini, and R. Cote, Phys. Rev. Lett. **95**, 223002 (2005).
[32] M. Yasuda, T. Kishimoto, M. Takamoto, and H. Katori, Phys. Rev. A **73**, 011403(R) (2006).
[33] A. Stein, H. Knöckel, and E. Tiemann, Phys. Rev. A **78**, 042508 (2008).
[34] G. Ferrari, R. E. Drullinger, N. Poli, F. Sorrentino, and G. M. Tino, Phys. Rev. A **73**, 023408 (2006).
[35] N. Poli, R. E. Drullinger, G. Ferrari, J. Léonard, F. Sorrentino, and G. M. Tino, Phys. Rev. A **71**, 061403 (R) (2005).
[36] S. B. Nagel, C. E. Simien, S. Laha, P. Gupta, V. S. Ashoka, and T. C. Killian, Phys. Rev. A **67**, 011401(R) (2003).
[37] P. G. Mickelson, Y. N. Martinez de Escobar, P. Anzel, B. J. DeSalvo, S. B. Nagel, A. J. Traverso, M. Yan, and T. C. Killian, J. Phys. B (to be published).
[38] M. Yasuda and H. Katori, Phys. Rev. Lett. **92**, 153004 (2004).
[39] T. Loftus, J. R. Bochinski, and T. W. Mossberg, Phys. Rev. A **66**, 013411 (2002).
[40] T. Ido, Y. Isoya, and H. Katori, Phys. Rev. A **61**, 061403 (R) (2000).
[41] K. M. O'Hara, M. E. Gehm, S. R. Granade, and J. E. Thomas, Phys. Rev. A **64**, 051403(R) (2001).
[42] S. Friebel, C. D'Andrea, J. Walz, M. Weitz, and T. W. Hänsch, Phys. Rev. A **57**, R20 (1998).
[43] C. J. Pethick and H. Smith, *Bose-Einstein Condensation in Dilute Gases* (Cambridge University Press, Cambridge, U.K., 2008).
[44] F. Dalfovo, S. Giorgini, L. P. Pitaevskii, and S. Stringari, Rev. Mod. Phys. **71**, 463 (1999).
[45] Y. Castin and R. Dum, Phys. Rev. Lett. **77**, 5315 (1996).